

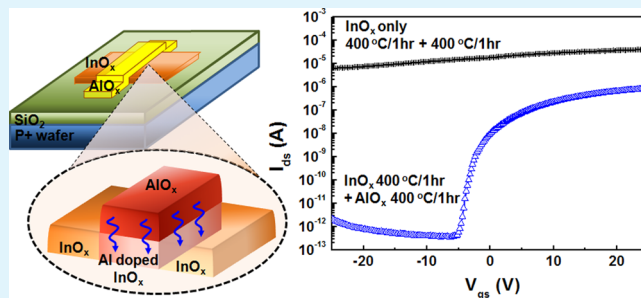
Homojunction Solution-Processed Metal Oxide Thin-Film Transistors Using Passivation-Induced Channel Definition

Jung Hyun Kim, You Seung Rim, and Hyun Jae Kim*

School of Electrical and Electronic Engineering, Yonsei University, 50 Yonsei-ro, Seodaemun-gu, Seoul 120-749, Republic of Korea

ABSTRACT: A simple method of channel passivation and physical definition of solution-processed metal oxide thin-film transistors (TFTs) has been developed for aluminum oxide (AlO_x) and indium oxide (InO_x) thin films. A photoresist-free-based ultraviolet (UV) patterning process was used to define an InO_x layer as the source/drain region and an AlO_x layer as a passivation layer on the InO_x layer. The Al diffused into the patterned InO_x thin film during a thermal annealing step. As an electrode, the patterned InO_x thin film had low resistivity, and as a channel, the Al-diffused InO_x thin film had a low carrier concentration. Furthermore, the diffused Al behaved as a carrier suppressor by reducing oxygen vacancies within the InO_x thin film. We succeeded in forming a coplanar homojunction-structured metal oxide TFT that used the passivation-induced channel-defining (PCD) method with an $\text{AlO}_x/\text{InO}_x$ bilayer. The PCD TFT had a field-effect mobility of $0.02 \text{ cm}^2/\text{V}\cdot\text{s}$, a threshold voltage of -1.88 V , a subthreshold swing of $0.73 \text{ V}/\text{decade}$, and an on/off current ratio of 2.75×10^6 with a width/length (W/L) of $2000 \mu\text{m}/400 \mu\text{m}$.

KEYWORDS: thin-film transistors, aluminum oxide, indium oxide, coplanar homojunction



1. INTRODUCTION

Since the discovery of amorphous InGaZnO as a semi-conducting material by Hosono et al. in 2004,¹ metal oxide semiconductors have attracted a great deal of attention as a channel material. Metal oxide semiconductor-based thin-film transistors (TFTs) have advantages such as high mobility ($\sim 10 \text{ cm}^2/\text{V}\cdot\text{s}$) with good electrical uniformity for large area deposition and high transparency in visible light. For these reasons, they have emerged as candidates for next-generation liquid-crystal displays and organic light-emitting diode displays. Metal oxide semiconductor films can be formed by various techniques such as pulse laser deposition,² atomic layer deposition,³ sputtering,⁴ and solution processing.⁵ Among these methods, the solution process has many advantages, including nonvacuum processing, selective deposition, and low cost. However, it requires the use of conventional photolithography for patterning. By using a photoresist (PR)-free-based ultraviolet (UV) patterning process with photosensitive solutions, we achieved a much simpler process than the conventional patterning process, as reported previously.⁶

Many studies have reported using homojunction-structured metal oxide TFTs.^{7–9} These structures had good electrical performance. Two approaches are generally used for their manufacture. One uses a plasma treatment to define the electrodes,^{7,8} and the other applies transparent conducting oxide source/drain electrodes on the channel with the homojunction material.⁹ Typically, these methods require an additional process, such as photolithography and specific metallization, which adds cost and complexity to the TFT fabrication. Here, we report a simple process to form coplanar

homojunction-structured aluminum oxide (AlO_x)/indium oxide (InO_x) bilayer TFTs using a passivation-induced channel-defining (PCD) method. Each layer was formed by a solution-based process via a PR-free-based UV patterning method.

2. EXPERIMENTAL PROCEDURE

Figure 1a is a schematic diagram of the PCD TFT discussed here. To fabricate this structure, separate solutions were used to make the InO_x and AlO_x layers. A 0.3 M solution of InO_x was prepared by dissolving indium nitrate hydrate [$\text{In}(\text{NO}_3)_3 \cdot x\text{H}_2\text{O}$] in 2-methoxyethanol ($\text{C}_3\text{H}_8\text{O}_2$, 2ME). A 0.3 M solution of AlO_x was prepared by dissolving aluminum nitrate hydrate [$\text{Al}(\text{NO}_3)_3 \cdot 9\text{H}_2\text{O}$] in 2ME. Benzoylacetone ($\text{C}_{10}\text{H}_{10}\text{O}_2$, BzAc) was used to photosensitize the two metal oxide solutions.^{10–12} It was mixed separately into the InO_x solution at a 1:1 molar ratio (In/BzAc) and into the AlO_x solution also at a 1:1 molar ratio (Al/BzAc). The process flowchart, including PR-free-based UV patterning, is shown in Figure 1b. The BzAc/ InO_x solution was spin-coated on $\text{SiO}_2/\text{p}^+\text{-doped Si}$, in which SiO_2 was used as the gate insulator and $\text{p}^+\text{-doped Si}$ was used as the gate. The spin coating was done at 3000 rpm for 30 s. The coated substrate was then soft-baked for 90 s at $130 \text{ }^\circ\text{C}$ and irradiated by a UV lamp for 15 min with a line-patterned mask to provide a source/drain width of $2000 \mu\text{m}$. After irradiation, the source/drain mask was removed and the substrate was leached in 2ME for 1 min. The irradiated region did not dissolve in 2ME. The UV-patterned InO_x layer was annealed for 1 h at $400 \text{ }^\circ\text{C}$ in ambient air. The BzAc/ AlO_x solution was then spin-coated onto the InO_x layer at 1500 rpm for 30 s. The UV irradiation process was

Received: December 13, 2013

Accepted: March 10, 2014

Published: March 10, 2014

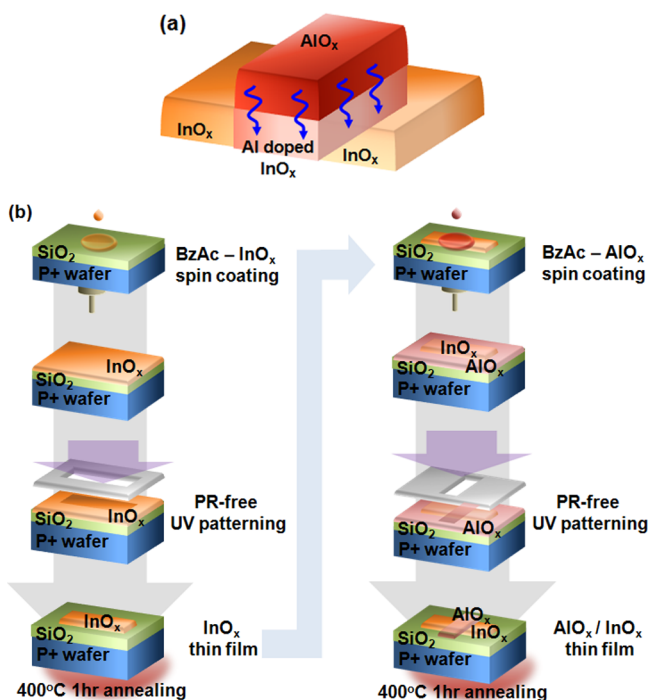


Figure 1. (a) Schematic diagram of a PCD TFT. (b) Formation of PCD TFTs.

repeated with a line-patterned mask of width $400\ \mu\text{m}$ to define the channel/passivation. After the leaching process, the patterned AlO_x layer was annealed for 1 h at $400\ ^\circ\text{C}$ in air. The PCD TFT was fabricated in this manner ($W/L = 2000\ \mu\text{m}/400\ \mu\text{m}$). A Hall effect measurement system (Ecopia HMS-3000) and a semiconductor analyzer (Agilent 4145B) were used to measure the electrical properties of the PCD TFT at room temperature. In the fabricated structure, the InO_x layer was annealed twice, i.e., during formation of both the InO_x and AlO_x layers. Thus, the reference samples used for measuring the InO_x layer only were also annealed twice. The gate voltage (V_{gs}) was swept from -25 to $+25$ V, and the drain voltage (V_{ds}) was applied at a constant 10.1 V for the transfer curve measurement. For the output curve measurement, V_{ds} was swept from 0 to 25 V, and V_{gs} varied from 0 to 25 V in 5 V increments. X-ray photoelectron spectroscopy (XPS) data were acquired in depth-profile mode with $1\ \text{keV}$ Ar^+ -ion sputtering.

3. RESULTS AND DISCUSSION

During PR-free-based UV patterning, π - π^* transitions occurred in InO_x and AlO_x complexes that had been formed

Table 1. Carrier Concentrations and Resistivities of InO_x and Al-Diffused InO_x Thin Films as a Function of the Annealing Temperature

| | 400 °C annealing | | 500 °C annealing | |
|----------------------------|--|------------------------------------|--|------------------------------------|
| | carrier concentration (cm^{-3}) | resistivity ($\Omega\text{-cm}$) | carrier concentration (cm^{-3}) | resistivity ($\Omega\text{-cm}$) |
| InO_x | 8.19×10^{18} | 2.08×10^{-1} | 4.45×10^{19} | 2.09×10^{-2} |
| Al-diffused InO_x | 3.18×10^{16} | 3.68×10^4 | 1.24×10^{18} | 1.48×10^0 |

in the presence of the added BzAc photosensitizer. The chelate bonding was decomposed in these solutions during UV irradiation. Hydrolysis and condensation reactions also occurred.^{6,10–12} The UV-irradiated and nonirradiated regions

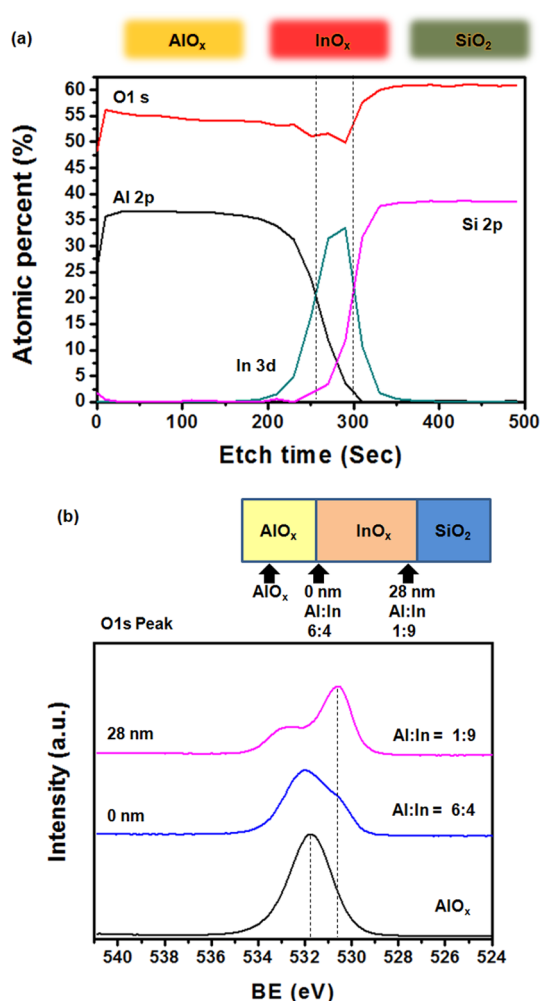


Figure 2. XPS data of the $400\ ^\circ\text{C}$ -annealed PCD structure. (a) Depth profile and (b) O 1s data as a function of the depth within the InO_x layer.

had very different solubilities in 2ME; i.e., the irradiated regions were insoluble.

Table 1 lists the Hall effect data for the InO_x and Al-diffused InO_x thin films for different annealing temperatures. For use as an electrode, an InO_x thin film must have a high carrier concentration and low resistivity. The carrier concentration decreased and the resistivity increased with decreasing annealing temperature of the InO_x thin film. For annealing above $400\ ^\circ\text{C}$, the InO_x thin film showed the electrical characteristics of an electrode. The channel layer could be affected by diffusion of a capping material, and this diffusant could control the electric characteristics of the channel.¹³ A lower carrier concentration, i.e., $< \sim 10^{17}\ \text{cm}^{-3}$, and a higher resistivity than the electrode are needed to use an Al-diffused InO_x thin film as a channel.¹⁴ Typically, a high annealing temperature is required to obtain excellent electrical properties when the solution process is used. It is essential to use the proper annealing temperature to control Al-ion diffusion in the PCD process. An Al-diffused InO_x thin film annealed at $500\ ^\circ\text{C}$ was not suitable as a channel because the carrier concentration was higher than that of a $400\ ^\circ\text{C}$ -annealed thin film. The carrier concentration and resistivity of the Al-diffused InO_x thin film were $3.18 \times 10^{16}\ \text{cm}^{-3}$ and $3.68 \times 10^4\ \Omega\text{-cm}$ for an annealing temperature of $400\ ^\circ\text{C}$. The InO_x and Al-diffused InO_x thin

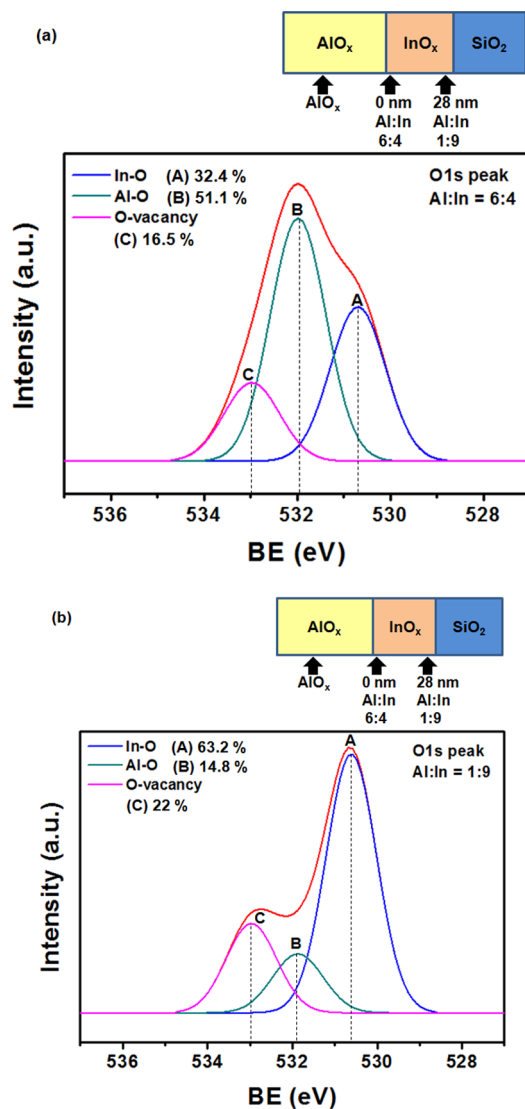


Figure 3. O 1s XPS data of the 400 °C-annealed AlO_x/InO_x structure: (a) Al:In = 6:4; (b) Al:In = 1:9.

films could be used as an electrode and a channel when they were annealed at 400 °C because they had acceptable carrier concentrations and resistivities.

XPS depth profiling of the PCD TFT fabricated at 400 °C provided evidence of Al diffusion in the InO_x thin film (Figure 2a). The In 3d peak appeared after 250–300 s of sputtering, and the Al 2p peak showed a gradient distribution in the InO_x layer. A large amount of the Al diffused into the InO_x layer during the postannealing step of AlO_x layer formation. Figure 2b shows the O 1s XPS spectrum as a function of the position within the InO_x layer. The O 1s peak of AlO_x was observed at ~532 eV, and the O 1s peak within the InO_x layer showed the harmonic peaks of AlO_x and InO_x.¹⁵ For a more detailed analysis, the O 1s spectra within the InO_x layer were deconvoluted using Gaussian distributions of three components centered at 530.6, 531.9, and 533 eV (Figure 3). Region A, having the lowest binding energy (BE), corresponds to O²⁻ ions associated with neighboring In atoms.¹⁶ Region B, having mid-range BE, corresponds to O²⁻ ions associated with neighboring Al atoms.¹⁷ Region C, with the highest BE, corresponds to O²⁻ ions in oxygen-deficient environments.¹⁶ The relative areas of regions A and B changed with the Al:In

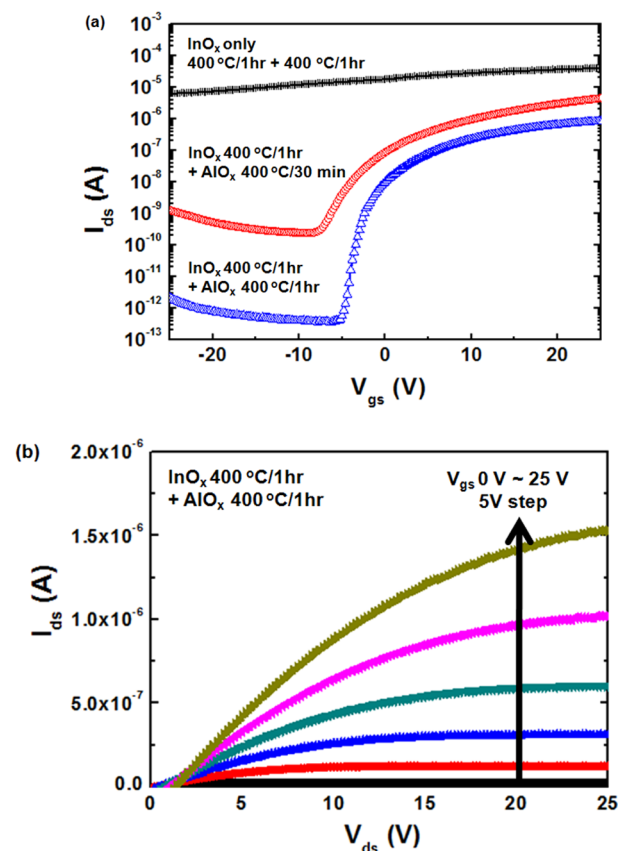


Figure 4. (a) Transfer curve of PCD TFTs as a function of the annealing time for AlO_x formation at 400 °C. (b) Output characteristics of PCD TFTs with AlO_x annealed for 1 h at 400 °C.

ratio in InO_x. As this ratio decreased from 6:4 to 1:9, the area of A increased from 32.4 to 63.2%, and the area of B decreased from 51.1 to 14.8%. The area of C increased from 16.5 to 22% as the Al:In ratio decreased. This result implied that the diffused Al reduced the oxygen deficiency with respect to oxygen vacancies (V_O) in the InO_x layer. Al has a lower standard electrode potential (SEP) than In (Al, $-1.662E^{\circ}/V$; In, $-0.4E^{\circ}/V$). Low-SEP materials, such as zirconium,¹⁸ lanthanum,¹⁹ yttrium,²⁰ and hafnium,²¹ are well-known as V_O-suppressing materials in metal oxides. A low SEP value means that the atom has a high tendency to lose electrons and to combine with oxygen molecules. Considering the strong oxidation characteristics of Al, diffused Al could remove V_O and V_O-related oxygen deficiencies in the channel layer via strong metal oxide bonding. In general, V_O is the major source of free carriers in metal oxide semiconductors;^{22,23} the reduction of V_O by Al diffusion leads to a decrease in the carrier concentration in the InO_x layer.

Figure 4a shows the transfer curve of the PCD TFT as a function of the annealing time for varying amounts of diffused Al. Without Al diffusion, the InO_x thin film exhibited conduction typical of an electrode. With application of an AlO_x layer onto the InO_x thin film and annealing, the transfer curve changed from conducting to semiconducting. Increasing the annealing time from 30 to 60 min at 400 °C improved the switching performance of the PCD TFT with an increased on/off current ratio. This indicated that the carrier concentration of the InO_x region could be suppressed underneath the AlO_x capping layer and that this phenomenon originated from the

diffusion of Al into InO_x . Furthermore, PCD TFTs offer advantages such as a passivation effect at the back-channel region via ambient as well as reduced degradation of the TFT performance due to reaction with H_2O molecules in air. An InO_x film without diffused Al showed electrode-like high conductivity. However, after annealing of AlO_x at 400°C for 60 min, the PCD TFT had a field-effect mobility of $0.02\text{ cm}^2/\text{V}\cdot\text{s}$, a threshold voltage of -1.88 V , a subthreshold swing of $0.73\text{ V}/\text{decade}$, and an on/off current ratio of 2.75×10^6 with a W/L of $2000\text{ }\mu\text{m}/400\text{ }\mu\text{m}$. As shown in Figure 4b, our PCD TFT showed a pinch-off and saturation behavior. This result is consistent with our transfer modulation by a AlO_x stacked InO_x TFT.

4. CONCLUSION

The fabrication of a solution-processed metal oxide TFT, having a coplanar homojunction structure consisting of an AlO_x and InO_x bilayer, using a PCD method has been demonstrated. The source/drain region was identified using a conductive InO_x layer without the conventional source/drain formation process that uses photolithography/etching. Thermal diffusion of Al into the InO_x layer occurred during annealing of the AlO_x layer. The diffused Al acted as a carrier suppressor, decreased the carrier concentration, and also defined the channel region. This simple and efficient method of selective Al diffusion enabled the fabrication of metal oxide TFTs. We expect that the upper AlO_x layer would enable back-channel passivation of the InO_x layer. These results also demonstrate the potential of PCD for the simple, cost-effective manufacture of metal oxide TFTs.

AUTHOR INFORMATION

Corresponding Author

*E-mail: hjk3@yonsei.ac.kr.

Author Contributions

J.H.K. and Y.S.R. contributed equally to this work.

Notes

The authors declare no competing financial interest.

ACKNOWLEDGMENTS

This work was supported by a National Research Foundation of Korea grant funded by the Korean Ministry of Education, Science and Technology (Grant 2011-0028819).

REFERENCES

- (1) Nomura, K.; Ohta, H.; Takagi, A.; Kamiya, T.; Hirano, M.; Hosono, H. Room-temperature fabrication of transparent flexible thin-film transistors using amorphous oxide semiconductors. *Nature* **2004**, *432*, 488–491.
- (2) Frenzel, H.; Lajn, A.; Brandt, M.; von Wenckstern, H.; Biehne, G.; Hochmuth, H.; Lorenz, M.; Grundmann, M. ZnO metal-semiconductor field-effect transistors with Ag-Schottky gates. *Appl. Phys. Lett.* **2008**, *92*, 192108.
- (3) Lim, S. J.; Kwon, S.; Kim, H.; Park, J.-S. High performance thin film transistor with low temperature atomic layer deposition nitrogen-doped ZnO. *Appl. Phys. Lett.* **2007**, *91*, 183517.
- (4) Martins, R.; Barquinha, P.; Ferreira, I.; Pereira, L.; Gonçalves, G.; Fortunato, E. Role of order and disorder on the electronic performances of oxide semiconductor thin film transistors. *J. Appl. Phys.* **2007**, *101*, 044505.
- (5) Kim, G. H.; Shin, H. S.; Ahn, B. D.; Kim, K. H.; Park, W. J.; Kim, H. J. Formation Mechanism of Solution-Processed Nanocrystalline InGaZnO Thin Film as Active Channel Layer in Thin-Film Transistor. *J. Electrochem. Soc.* **2009**, *156*, H7–H9.

- (6) Rim, Y. S.; Lim, H. S.; Kim, H. J. Low-Temperature Metal-Oxide Thin-Film Transistors Formed by Directly Photopatternable and Combustible Solution Synthesis. *ACS Appl. Mater. Interfaces* **2013**, *5*, 3565–3571.

- (7) Ahn, B. D.; Shin, H. S.; Kim, H. J.; Park, J.-S.; Jeong, J. K. Comparison of the effects of Ar and H_2 plasmas on the performance of homojunctioned amorphous indium gallium zinc oxide thin film transistors. *Appl. Phys. Lett.* **2008**, *93*, 203506.

- (8) Lin, H.-C.; Lyu, R.-J.; Hwang, T.-Y. Fabrication of High-Performance ZnO Thin-Film Transistors With Submicrometer Channel Length. *IEEE Electron Device Lett.* **2013**, *34*, 1160–1162.

- (9) Lavareda, G.; Nunes de Carvalho, C.; Fortunato, E.; Ramos, A. R.; Alves, E.; Conde, O.; Amaral, A. Transparent thin film transistors based on indium oxide semiconductor. *J. Non-Cryst. Solids* **2006**, *352*, 2311–2314.

- (10) Zhao, G.; Tohge, N.; Nishii, J. Fabrication and characterization of diffraction grating using photosensitive Al_2O_3 gel films. *Jpn. J. Appl. Phys.* **1998**, *37*, 1842–1846.

- (11) Li, Y.; Zhao, G.; Zhang, W.; Chen, Y. Using the photolysis of chemically modified gel films preparing ITO fine patterned thin films. *J. Display Technol.* **2006**, *2*, 175–179.

- (12) Tohge, N.; Shinmou, K.; Minami, T. Effects of UV-irradiation on the formation of oxide thin films from chemically modified metal-alkoxides. *J. Sol-Gel Sci. Technol.* **1994**, *2*, 581–585.

- (13) Zan, H.-W.; Yeh, C.-C.; Meng, H.-F.; Tsai, C.-C.; Chen, L.-H. Achieving High Field-Effect Mobility in Amorphous Indium–Gallium–Zinc Oxide by Capping a Strong Reduction Layer. *Adv. Mater.* **2012**, *24*, 3509–3514.

- (14) Hong, D.; Yerubandi, G.; Chiang, H. Q.; Spiegelberg, M. C.; Wager, J. F. Electrical Modeling of Thin-Film Transistors. *Crit. Rev. Solid State Mater. Sci.* **2008**, *33*, 101–132.

- (15) Won, S.-J.; Huh, M. S.; Park, S.; Suh, S.; Park, T. J.; Kim, J. H.; Hwang, C. S.; Kim, H. J. Capacitance and Interface Analysis of Transparent Analog Capacitor Using Indium Tin Oxide Electrodes and High- k Dielectrics. *J. Electrochem. Soc.* **2010**, *157*, G170–175.

- (16) Han, S.-Y.; Herman, G. S.; Chang, C. Low-Temperature, High-Performance, Solution-Processed Indium Oxide Thin-Film Transistors. *J. Am. Chem. Soc.* **2011**, *133*, 5166–5169.

- (17) Li, Y.; Wang, L. Study of oxidized layer formed on aluminium alloy by plasma oxidation. *Thin Solid Films* **2009**, *517*, 3208–3210.

- (18) Rim, Y. S.; Kim, D. L.; Jeong, W. H.; Kim, H. J. Effect of Zr addition on ZnSnO thin-film transistors using a solution process. *Appl. Phys. Lett.* **2010**, *97*, 233502.

- (19) Kim, D. N.; Kim, D. L.; Kim, G. H.; Kim, S. J.; Rim, Y. S.; Jeong, W. H.; Kim, H. J. The effect of La in InZnO systems for solution-processed amorphous oxide thin-film transistors. *Appl. Phys. Lett.* **2010**, *97*, 192105.

- (20) Shin, H. S.; Kim, G. H.; Jeong, W. H.; Ahn, B. D.; Kim, H. J. Electrical Properties of Yttrium–Indium–Zinc-Oxide Thin Film Transistors Fabricated Using the Sol–Gel Process and Various Yttrium Compositions. *Jpn. J. Appl. Phys.* **2010**, *49*, 03CB01.

- (21) Jeong, W. H.; Kim, G. H.; Kim, D. L.; Shin, H. S.; Kim, H. J.; Ryu, M.-K.; Park, K.-B.; Seon, J.-B.; Lee, S.-Y. Effects of Hf incorporation in solution-processed Hf-InZnO TFTs. *Thin Solid Films* **2011**, *519*, 5740–5743.

- (22) Luo, S. N.; Kono, A.; Noguchi, N.; Shoji, F. Effective creation of oxygen vacancies as an electron carrier source in tin-doped indium oxide films by plasma sputtering. *J. Appl. Phys.* **2006**, *100*, 113701.

- (23) Kim, G. H.; Jeong, W. H.; Ahn, B. D.; Shin, H. S.; Kim, H. J.; Kim, H. J.; Ryu, M.-K.; Park, K.-B.; Seon, J.-B.; Lee, S.-Y. Investigation of the effects of Mg incorporation into InZnO for high-performance and high-stability solution-processed thin film transistors. *Appl. Phys. Lett.* **2010**, *96*, 163506.